American Journal of Innovation in Science and Engineering (AJISE)

ISSN: 2158-7205 (ONLINE)

VOLUME 4 ISSUE 3 (2025)

PUBLISHED BY
E-PALLI PUBLISHERS, DELAWARE, USA

American Journal of Innovation in Science and Engineering (AJISE)

Volume 4 Issue 3, Year 2025
ISSN: 2158-7205 (Online)
DOI: https://doi.org/10.54536/ajise.v4i3.5836
https://journals.e-palli.com/home/index.php/ajise

Blockchain-Enabled Nanocatalyst Monitoring System for Real-Time Dye Degradation in Industrial Wastewater

Echezona Uzoma[1], Onuh Matthew Ijiga[2*], Sombo Terver[2], Jubu Peverga[2]

Article Information

Received: August 17, 2025
Accepted: September 20, 2025
Published: November 06, 2025

Keywords

Blockchain, Environmental Monitoring, Dye Degradation, Nanocatalyst, Wastewater Treatment

ABSTRACT

The environmental and regulatory problems caused by industrial wastewater containing synthetic dyes such as methylene blue become more complex because these substances remain toxic and persistent while showing resistance to standard biological treatment methods. The research describes the creation of a blockchain-enabled nanocatalyst tracking system that detects and verifies dye pollutants in water streams through real-time monitoring. The system uses semiconductor nanocatalysts with advanced oxidation processes to break down, and uses microcontrollers to process data signals before blockchain protocols store performance metrics, which maintain transparency and immutability, and meet worldwide environmental reporting requirements. The system included a miniaturized reactor chamber with automated fluid management pollutants efficiently while optical and electrochemical sensors track concentration changes and monitor pH and temperature levels. The system and wireless blockchain connectivity in its compact design. The system achieved 85% methylene blue degradation in controlled tests while sensor data showed pseudo-first-order kinetics and maintained high calibration stability. The system performed well in power efficiency tests while showing fast blockchain transaction speeds and it maintained stability through different operational settings. The cost evaluation showed that the system operates within budget while environmental studies demonstrated better carbon emission performance than traditional monitoring systems. The proposed framework combines nanocatalytic water treatment with blockchain-based data tracking to create a sustainable wastewater management system which works for municipal treatment facilities and industrial sites and decentralized monitoring systems. The integration of environmental nanotechnology with digital compliance systems through this innovation enables the development of self-regulating water treatment systems for the next generation.

INTRODUCTION

Textile, pharmaceutical, and chemical industrial wastewater contains persistent organic pollutants, where the most dangerous and carcinogenic methylene blue dye, along with other synthetic dyes, causes harm to aquatic life by blocking light-resistant groups (Forgacs *et al.*, 2004). The toxic and non-biodegradable and penetration and photosynthesis (Crini, 2006). The stable aromatic structures of these dyes make them impossible for microbial systems to break down during biological treatment processes (Robinson *et al.*, 2001). The two most challenging dye categories are azo and cationic dyes because their chromophores show resistance to oxidative breakdown which results in the creation of potentially carcinogenic amines during incomplete decomposition (Ali, 2010; Kant, 2012).

The remediation methods of coagulation–flocculation and membrane separation and adsorption face major drawbacks because they produce large amounts of sludge and experience fouling issues and require expensive regeneration processes (Bielska & Szymanowski, 2006). The insufficient performance of current catalytic degradation methods has led to increased interest in using nanostructured catalysts for heterogeneous photocatalysis and advanced oxidation processes (AOPs) to break down dyes into safer substances (Rauf & Ashraf, 2009). The current monitoring systems for catalytic degradation face significant limitations despite recent progress in degradation technology. Supervisory control systems that monitor treatment performance depend on periodic sampling and laboratory testing of data which gets stored in centralized databases that face security risks (Katheresan *et al.*, 2018; Zhang *et al.*, 2020). Real-time process control and regulatory compliance traceability become impossible because of this limitation.

Real-time sensing platforms that use blockchain technology create a revolutionary solution to solve these problems. The combination of blockchain technology with decentralized logging at sensor level provides secure data protection and complete auditability and transparent treatment performance monitoring (Clohessy *et al.*, 2020; Kouhizadeh *et al.*, 2021). The research introduces a blockchain-based nanocatalyst monitoring system which tracks dye degradation processes. The research aims to (i) create a nanocatalytic degradation system with built-in sensors and (ii) create blockchain protocols for transparent compliance reporting and (iii) test the system's wastewater treatment performance under controlled conditions and (iv) evaluate its operational scalability and economic viability and environmental advantages.

[1] Information Technology Solutions & Product Development Branch, Ministry of Public and Business Service Delivery and Procurement, Toronto, Ontario, Canada
[2] Department of Physics, Joseph Sarwaan Tarkaa University, Makurdi, Benue State, Nigeria
[*] Corresponding author's e-mail: onuhijiga@gmail.com

LITERATURE REVIEW

Advanced Oxidation Processes and Nanocatalysts in Wastewater Treatment

The chemical treatment technology of Advanced Oxidation Processes (AOPs) uses hydroxyl radicals (•OH) with 2.8 V oxidation potential to remove persistent organic pollutants (POPs) from wastewater. The non-selective radicals in AOPs effectively break down complex dye structures which show resistance to standard biological and physical-chemical treatment methods. The four main AOP technologies include photocatalysis and Fenton and photo-Fenton reactions and ozonation and electrochemical oxidation which can be optimized for different wastewater types based on pH levels and contaminant amounts and energy requirements (Oturan & Aaron, 2014). The use of semiconductor nanomaterials TiO_2, ZnO and Fe_3O_4 in heterogeneous photocatalysis has become popular because they offer high surface area-to-volume ratios and adjustable band gaps and light activation under UV or visible light. The nanocatalysts produce electron–hole pairs when exposed to light which leads to redox reactions that break down chromophoric dye structures into CO_2 and H_2O. Nanocatalyst performance under real wastewater conditions has improved through recent advancements in doping methods and core–shell design and surface modification techniques (Khan *et al.*, 2021). The combination of nanocatalysts with continuous-flow treatment systems including membrane reactors and packed-bed photoreactors and microfluidic devices enhances process intensification through better photon utilization and mass transfer. Nanocatalysts that receive surface modification with silica and carbon nanotubes and polymeric membranes show better lifecycle performance and regulatory compliance because they prevent aggregation and leaching. Nanocatalytic AOPs achieve dye removal rates above 90% when treating methylene blue and crystal violet and Congo red solutions through irradiation processes that depend on catalyst amount and dye concentration and light power (Rajamanickam & Shanthi, 2016). The operational success of nanocatalytic AOPs depends heavily on solution pH levels and ionic strength and the presence of radical scavengers. The deployment of integrated sensing platforms for real-time degradation kinetic monitoring becomes necessary to optimize system performance and achieve reproducible results. The sensors need to establish perfect connections with control systems and data logging systems for accurate treatment performance measurement in regulatory environments. The research develops an AOP-based nanocatalyst system which includes real-time data collection and blockchain-based tracking mechanisms.

Sensor Technologies for Dye Monitoring

The monitoring of wastewater treatment dye degradation requires sensors which detect dye concentration and physicochemical changes in real time with high precision and selectivity and stability. The main analytical tool for detecting synthetic dyes, including methylene blue, crystal violet, and azo derivatives, uses optical sensors that operate through absorbance spectroscopy. The Beer–Lambert law enables concentration tracking of dyes through their characteristic absorbance peaks which occur between 200–800 nm in the visible or UV-visible range. The combination of photodiodes or phototransistors with optoelectronic systems results in compact low-power devices which work well for embedded applications (Hassan & Shakaff, 2016). The detection of redox-active intermediates produced during dye breakdown becomes possible through electrochemical sensors which include amperometric and potentiometric and voltametric configurations. The construction of sensors with nanostructured electrodes made from graphene and gold nanoparticles and carbon nanotubes enables high surface area and fast electron transfer rates. The electrochemical investigation of dyes and their breakdown products through cyclic voltammetry and differential pulse voltammetry enables researchers to develop kinetic and mechanistic models for catalytic processes (Sadeghi *et al.*, 2019). The integration of these sensors into microfluidic platforms enables real-time process control for continuous flow systems through miniaturization. The combination of sensor fusion with wireless communication technology has enabled the creation of multisensor arrays that unite optical and electrochemical measurements with environmental parameters including pH and conductivity and temperature to monitor complete catalytic performance and effluent quality. The systems use embedded microcontrollers together with analog-to-digital converters to process signals before sending data to distributed or centralized control systems. The accuracy of sensor networks improves through built-in calibration algorithms and signal filtering and drift compensation protocols. The deployment of sensors in chemically aggressive environments requires sensor housings made from inert materials including polytetrafluoroethylene (PTFE) and stainless steel and epoxy composites (Yadav *et al.*, 2021). Sensor-generated data streams function as the base information for blockchain-enabled monitoring systems to execute smart contracts while maintaining system credibility and regulatory trust through reliable sensor operations and precise measurements.

Blockchain Applications in Environmental Monitoring

The environmental monitoring sector uses blockchain technology to create systems which protect data integrity while enabling full traceability and complete transparency. The centralized nature of SCADA and CMMS frameworks makes them vulnerable to data manipulation and unauthorized access and system breakdowns. The decentralized nature of blockchain technology enables secure time-stamped event recording through distributed ledgers that exist across multiple nodes to protect environmental data from tampering. The distributed system design of blockchain technology strengthens monitoring system reliability because it

provides essential data log immutability and verifiability needed for regulatory compliance (Clohessy *et al.*, 2020). The implementation of blockchain technology in wastewater management enables the tracking of chemical emissions and treatment performance and pollutant concentration changes throughout time. The combination of environmental sensors with blockchain smart contracts enables automatic data validation and recording of field device readings including pH and COD and dye concentration measurements without needing central authority supervision. Smart contracts within the system perform automated policy enforcement through predefined rules which detect threshold breaches and activate maintenance notifications for environmental policy compliance (Kouhizadeh *et al.*, 2021). The system design enables third-party regulators to verify pollutant degradation events through auditable workflows which eliminate trust asymmetries in environmental governance. The standardization of data exchange formats through JSON and MQTT and OPC-UA enables blockchain to connect different monitoring devices and enterprise systems. The implementation of Ethereum sidechains and permissioned frameworks like Hyperledger Fabric addresses computational limitations and sensor network latency problems in recent blockchain deployments. The system configurations enable embedded devices with limited power to join blockchain-based logging operations without performance degradation. The system integrates wastewater treatment sensors to log and hash dye degradation data including absorbance spectra and catalytic chamber temperature measurements at scheduled intervals (Reyna *et al.*, 2018).

Gaps in Existing Technologies and Research

The current dye degradation methods and environmental monitoring systems have achieved progress yet they still need improvement in their integration capabilities and operational reliability and scalability. The conventional dye degradation methods including adsorption and membrane filtration and classical AOPs do not have built-in systems for real-time process monitoring or automated system optimization. The methods operate through batch processes which require extensive human effort and fail to adjust their performance when wastewater composition changes or operational parameters shift. The absence of sensor systems that deliver precise continuous chemical analysis of degradation processes makes it challenging to evaluate their performance (Wang *et al.*, 2018). The digital framework of wastewater treatment facilities shows a major separation between sensor information collection and protected data handling systems. Sensor networks function independently from each other because they operate without standard interoperability protocols and maintain insufficient backup systems. The fragmented system structure hampers both predictive maintenance operations and regulatory reporting transparency. The lack of cryptographic verification in proprietary data formats used by these systems makes their recorded information susceptible to loss or unauthorized changes or tampering particularly in areas with weak environmental compliance enforcement or political instability (Zhao *et al.*, 2021). The current research shows an inadequate connection between nanoscale degradation platforms with high resolution and decentralized digital validation systems. Nanocatalysts show outstanding performance in degrading persistent dyes through solar or UV light exposure but researchers typically test them under controlled laboratory conditions. The experimental systems used for testing lack built-in diagnostic tools and real-world environmental factors and catalyst performance and stability monitoring systems. The research on catalytic materials at a fundamental level does not match the requirements of industrial-scale deployments because there are no verifiable data pipelines in place (Li *et al.*, 2020). The absence of connection between advanced sensing systems and catalytic degradation and blockchain technology enables the creation of autonomous platforms, which offer self-regulation, auditability, and operational flexibility. The solution to this knowledge gap demands interdisciplinary research that combines materials science with embedded electronics and decentralized computing to develop intelligent systems which track environmental changes and document their operational history. The integration of wastewater treatment solutions with smart infrastructure programs and international sustainability goals requires this essential convergence.

MATERIALS AND METHODS

Design of the Monitoring System Architecture

The blockchain-integrated nanocatalyst monitoring system operates through an embedded cyber-physical framework that unites sensor arrays with microcontroller-based signal processing and nanocatalytic degradation chambers and blockchain-enabled data logging modules. The device operates continuously to monitor dye concentration changes through its embedded intelligent system which performs autonomous operations while maintaining secure cryptographic data management.

The system consists of five interconnected components which include sensors and MCU and catalytic degradation chamber and power system and blockchain logging module as shown in Figure 1.

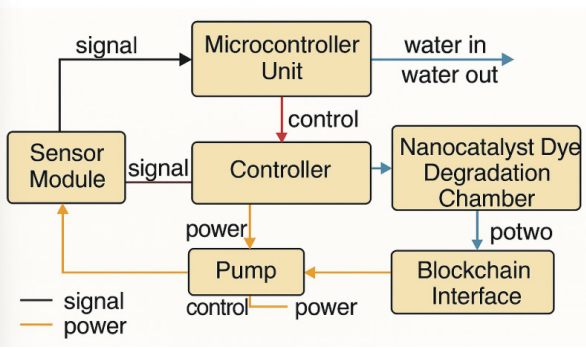

Figure 1: Block Diagram of the Overall System Architecture

The nanocatalytic degradation chamber operates to break down synthetic dyes including methylene blue through photocatalytic or redox reactions in water solutions. The chamber design promotes laminar flow while allowing photons to penetrate deeply and enabling optimal contact between catalysts and pollutants. The residence time of dye molecules within the chamber, τ, is given by:

$\tau = V/Q$

where V is the internal volume of the reaction chamber (m^3), and Q is the volumetric flow rate (m^3/s). The kinetics of dye degradation are modeled using pseudo-first-order reaction assumptions, where the rate of degradation follows:

$dC/dt = -kC$

Solving this yields:

$C(t) = C_0 e^{(-kt)}$

where C(t) is the dye concentration at time t, C_0 is the initial concentration, and k is the apparent reaction rate constant, influenced by catalyst surface area, photon flux, and pollutant diffusion dynamics.

The sensor module comprises a calibrated optical sensor array with a specific response at λ = 664 nm, the absorbance peak of methylene blue. The absorbance, A, is measured via Beer–Lambert's Law:

$A = \varepsilon \cdot l \cdot C$

where ε is the molar absorptivity ($L \cdot mol^{-1} \cdot cm^{-1}$), l is the optical path length (cm), and C is the molar concentration (mol/L). This enables precise, non-invasive quantification of dye concentration, which is then digitized and processed by the microcontroller.

The electrical subsystem includes a voltage regulator, analog front-end circuits, and a microcontroller (e.g., STM32 or Arduino Mega) to process sensor signals. A MOSFET switch controlled via a PWM signal regulates a peristaltic or diaphragm pump that circulates the dye solution. The power consumption of the system, P, is defined as:

$P = V \cdot I = V_{cc} \cdot I_{avg}$

where V_{cc} is the supply voltage and I_{avg} is the average current drawn by the system during operation. Optimization of energy usage is critical for mobile and off-grid deployments.

The blockchain interface is implemented via an ESP32 or Raspberry Pi module, communicating with a lightweight Ethereum-based smart contract or Hyperledger Fabric node. Each data packet from the sensor module is timestamped and hashed using a secure SHA-256 function:

$H(x) = SHA\text{-}256(x)$

where x is the concatenated string of sensor readings and system metadata. The hash is broadcast to a distributed ledger, ensuring traceability and non-repudiation.

The system functions through a state machine system which includes idle, monitoring, degrading, logging and fault recovery states. The system enters each state automatically through real-time sensor data and threshold rules that exist within the firmware. The system provides both environmental remediation capabilities and secure auditability through its direct connection between physical breakdown and cryptographic data authentication processes.

Theoretical Modeling of Dye Degradation Kinetics

The theoretical modeling of nanocatalyst-driven dye degradation in industrial wastewater combines knowledge from reaction kinetics and photophysics and electrochemistry and fluid dynamics. The photocatalytic decomposition of methylene blue (MB) under controlled illumination and constant catalyst concentration follows a pseudo-first-order kinetic model which can be described by the integrated rate equation:

$C_t = C_0 e^{(-kapp\ t)}$

where:

C_t is the dye concentration at time t,

C_0 is the initial dye concentration,

k_{app} is the apparent first-order rate constant (min^{-1}),

t is time (min).

The system's degradation efficiency at any point in time is calculated as:

$\eta(\%) = ((C_0\text{-}C_t)/C_0) \times 100$

Photocatalytic activity, particularly in nanomaterials like TiO_2, ZnO, or doped variants, involves photon-induced generation of electron-hole pairs. The rate of charge carrier generation G under illumination is modeled by:

$G = \alpha I_0 (1\text{-}R) e^{(-\alpha x)}$

Where,

α is the absorption coefficient (cm^{-1}),

I_0 is the incident light intensity (W/cm^2),

R is surface reflectance,

x is photon penetration depth (cm).

Carrier recombination and transport dynamics within the semiconductor follow the continuity equations based on Fick's second law:

$\partial n/\partial t = D_n (\partial^2 n)/(\partial x^2) - ((n\text{-}n_0))/\tau_n$, $\partial p/\partial t = D_p (\partial^2 p)/(\partial x^2) - ((p\text{-}p_0))/\tau_p$

where:

n and p are the time-dependent concentrations of electrons and holes, respectively,

D_n and D_p are their respective diffusion coefficients (cm^2/s),

n_0 and p_0 are equilibrium carrier concentrations,

τ_n and τ_p are carrier lifetimes (s).

To monitor degradation progress, optical measurements rely on the Beer-Lambert Law, which relates absorbance A to concentration:

$A = \varepsilon l C$

Where,

A is the absorbance (unitless),

ε is the molar absorptivity ($L \cdot mol^{-1} \cdot cm^{-1}$),

l is the optical path length (cm),

C is the dye concentration (mol/L).

The transport of fluid through the catalytic system crucial for maintaining residence time and reactant mixing is described using Bernoulli's equation:

$P_1 + 1/2\ \varrho v^2_1 + \varrho g h_1 = P_2 + 1/2\ \varrho v^2_2 + \varrho g h_2 + h_f$

Where,
P is pressure (Pa),
ϱ is fluid density (kg/m³),
v is flow velocity (m/s),
g is gravitational acceleration (9.81 m/s²),
h is elevation head (m),
h_f represents frictional head loss.
The developed formulations form a complete multiscale system which describes how nanocatalysts affect dye breakdown through kinetic processes and photonic activation and charge movement and fluid dynamics. The system benefits from real-time optical sensing and blockchain-based data validation which improves environmental monitoring transparency and traceability.
The actual hardware wiring layout appears in Figure 2 which demonstrates the essential components including the microcontroller and sensor inputs and relay control and blockchain interface.

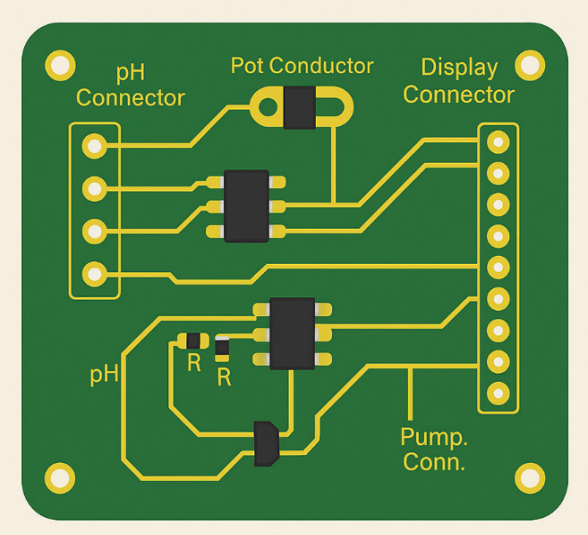

Figure 2: Labeled PCB Circuit Diagram

Signal Processing and Transduction Mechanisms in Sensor Integration

The dye degradation monitoring system operates with complete operational integrity because it uses efficient methods to acquire signals and amplify them before converting them into digital data from analog environmental readings. The system operates through electrochemical principles and photonics and analog circuit design and digital signal processing to achieve accurate real-time measurement and control.
The pH sensor functions based on the Nernst equation, which defines the electrochemical potential V_{pH} generated by an ion-selective electrode in response to hydrogen ion activity:

$$V_{pH} = V_0 - (2.303RT/F) \log_{10} [H^+]$$

Where,
V_0 is the standard electrode potential (V),
R is the universal gas constant (8.314 J·mol^{-1}·K^{-1}),
T is the absolute temperature (K),
F is Faraday's constant (96,485 C/mol),
$[H^+]$ is the hydrogen ion concentration (mol/L).
Temperature fluctuations are corrected through calibration routines that adjust the RT/F ratio, ensuring the electrochemical signal remains stable and accurate. The resulting analog voltage is conditioned through an operational amplifier (op-amp) in a non-inverting gain configuration:

$$V_{out} = V_{in} (1 + R_2/R_1)$$

where R_1 and R_2 are the input and feedback resistors, respectively. This stage ensures impedance matching and voltage scaling before digitization.
Simultaneously, the nanocatalyst-induced dye degradation is optically monitored via a photodiode or phototransistor that detects variations in absorbance. The photogenerated current I_{ph} is defined as:

$$I_{ph} = R_\lambda \cdot P_{opt}$$

where:
R_λ is the photodiode responsivity (A/W),
P_{opt} is the incident optical power (W).
This current is converted into a measurable voltage using a transimpedance amplifier:

$$V_{out} = -I_{ph} \cdot R_f$$

where R_f is the feedback resistor. The analog output is digitized by an n-bit Analog-to-Digital Converter (ADC) embedded in the microcontroller. The digital representation D is given by:

$$D = (2^n-1) \cdot (V_{in} / V_{ref})$$

To enhance signal clarity, embedded firmware applies digital filters typically a moving average filter to suppress high-frequency noise and fluctuations:

$$y[n] = \frac{1}{M} \sum_{k=0}^{M-1} x[n-k]$$

Where,
y[n] is the smoothed output,
x[n-k] represents previous signal samples,
M is the window size.
Hardware-level noise suppression is achieved through EMI shielding and the application of decoupling capacitors. These form passive low-pass filters with a cutoff frequency:

$$f_c = 1/2\pi RC$$

where R and C are the resistance and capacitance values, respectively. These filters attenuate high-frequency electromagnetic interference, preserving signal fidelity.
The multi-stage signal processing system provides reliable digital conversion of electrochemical and photonic signals through its sequential processing stages. The system data enables real-time system control and blockchain-based modules for transparent traceability and compliance reporting.

Thermodynamic and Kinetic Modeling of the Dye Degradation Process

The treatment of industrial dyes in wastewater systems through nanocatalysts depends on both thermodynamic reaction feasibility and the speed of chemical transformations. The process starts with dye

molecule adsorption onto TiO_2 or ZnO nanocatalysts under ambient or UV-irradiated conditions before redox reactions occur through hydroxyl radical (·OH) production from photocatalytic excitation.

The reaction spontaneity depends on the Gibbs free energy change (ΔG) which determines the thermodynamic feasibility of the process:

$$\Delta G = \Delta H - T\Delta S$$

Where,

ΔG is the Gibbs free energy change (J/mol),

ΔH is the enthalpy change (J/mol),

T is the absolute temperature (K),

ΔS is the entropy change (J/mol·K).

The reaction becomes spontaneous when ΔG shows a negative value. The photocatalytic dye oxidation process using UV-activated nanomaterials shows $\Delta G<0$ because photogenerated radicals possess strong oxidative properties.

Kinetically, the Langmuir–Hinshelwood (L–H) model offers a mechanistic description of the reaction rate r based on surface adsorption and subsequent catalytic conversion:

$$r = (k_r K_{ads} C_{dye})/(1 + K_{ads} C_{dye})$$

Where,

k_r is the intrinsic surface reaction rate constant ($mol \cdot L^{-1} \cdot s^{-1}$),

K_{ads} is the adsorption equilibrium constant (L/mol),

C_{dye} is the dye concentration in solution (mol/L).

The model bases its operation on dye molecules that adsorb as a single layer onto the catalyst surface which matches the physical adsorption patterns found in heterogeneous photocatalysis.

Under illumination, the photonic activation of the nanocatalyst results in the generation of electron-hole (e^-/h^+) pairs. The efficiency of this photoreaction is quantified through quantum efficiency η:

η = (“(number of dye molecules degraded)” ×(“electrons required per molecule”))/”number of incident photons”

The absorbed optical power that drives the photochemical reaction is given by:

$$P_{absorbed} = E \times A$$

Where,

E is the irradiance of the light source (W/m^2),

A is the effective illuminated surface area of the catalyst (m^2).

In steady-state operation, the net catalytic efficiency is determined by the competition between electron-hole pair generation and recombination, captured by the effective rate constant k_{eff}:

$$k_{eff} = k_{gen} - k_{rec}$$

Where,

k_{gen} is the generation rate constant of charge carriers,

k_{rec} is the recombination rate constant.

Optimizing k_{eff} is essential for maximizing the yield of reactive radicals and minimizing energy losses due to charge recombination.

The thermodynamic and kinetic models work together to establish the basis for reactor performance simulation and optimization. The system enables real-time process variable control through its models which also support sensor module integration and blockchain data transmission for regulatory compliance and system auditing.

Blockchain Integration and Cryptographic Hashing for Secure Data Transmission

The dye degradation monitoring system achieves real-time environmental data transmission through blockchain technology which provides secure tamper-proof and auditable operations. The system operates on a permissioned blockchain structure which enables decentralized verification of sensor data points that include absorbance (A) and dye concentration (C(t)) and pH values and timestamps (t). The system protects data integrity through cryptographic block encapsulation which provides tamper-evidence and traceability and data provenance to distributed validating nodes.

The system maintains data integrity through SHA-256 cryptographic hashing of structured messages M which contain concatenated sensor data entries.

$$H(M) = SHA\text{-}256(M)$$

The hash function demonstrates pre-image resistance and collision resistance and avalanche effect because any small modification to the input M produces a completely different hash output H(M) which protects transaction authenticity and uniqueness.

The integrity of data transmission is further enforced using Elliptic Curve Digital Signature Algorithm (ECDSA). Each node signs its hash output H(M) with a private key d, generating a digital signature (r,s). This signature is verified via the associated public key Q, using the elliptic curve verification condition:

$$s^{(-1)} (H(M) + r \cdot d) \equiv x \pmod n$$

Where,

$s^{(-1)}$ is the modular inverse of s,

r is the x-coordinate of the elliptic curve point used in signature generation,

d is the private signing key,

n is the order of the elliptic curve group,

x is the x-coordinate from the point verification computation.

Each new block B_i added to the blockchain follows a structured format:

$$B_i = \{Index_i, Timestamp_i, Data_i, H(B_{i-1}), H(B_i)\}$$

where:

$Index_i$ denotes the block’s position in the ledger,

$Timestamp_i$ records the transaction time,

$Data_i$ includes signed sensor values and metadata,

$H(B_{i-1})$) links to the previous block’s hash to maintain continuity,

$H(B_i)$ is the current block’s hash ensuring chain integrity.

The delegated consensus mechanism operates in embedded IoT applications to achieve energy efficiency while minimizing computational overhead because it replaces Proof-of-Work (PoW) method.

The energy consumed during each blockchain transaction is modeled as:

$$P_b = V \cdot I_b \cdot t_{tx}$$

Where,
V is the system's supply voltage (V),
I_b is the average current draw during transmission (A),
t_{tx} is the duration of each data transaction (s).
Transaction latency L_b, crucial for responsive system actuation, is computed by:
$L_b = T_{net} + T_{block}$
Where,
T_{net} represents network propagation delay,
T_{block} is the block validation time.
To minimize L_b and support real-time sensor-actuator feedback loops, the system employs lightweight communication protocols such as MQTT or LoRaWAN, which are optimized for low-bandwidth, energy-constrained environments.
The blockchain layer achieves end-to-end data security and verifiable compliance and transparent environmental governance through its integration of cryptographic hashing and digital signatures and consensus algorithms and power-aware transmission models.

Prototype Construction and Assembly
The blockchain-integrated nanocatalyst dye degradation monitoring system underwent a systematic engineering development process which emphasized performance alongside modularity and system resilience. The development process consisted of three main stages which involved selecting precise hardware components followed by making custom subsystems and integrating all components under controlled testing environments. The prototype system operated autonomously while performing real-time actions and maintaining secure cryptographic data recording.
Figure 3; Circuit diagram of the blockchain-enabled nano-catalyst monitoring system integrating pH sensing, OLED display, and automated fluid control via MOSFET-driven pump. The system is powered by a 9V battery and managed by an Arduino microcontroller.

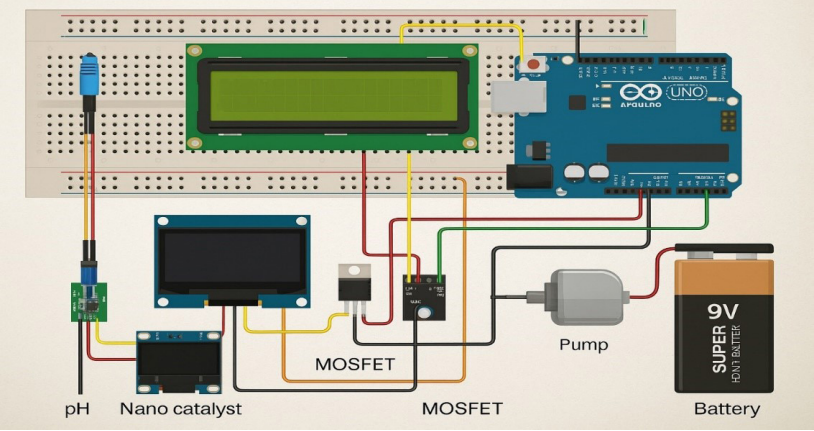

Figure 3: Circuit Diagram of Blockchain-Enabled Nano-Catalyst Monitoring System

The mechanical frame received design input from SolidWorks before its construction using precision laser-cut acrylic and polycarbonate materials for chemical resistance and structural strength. The borosilicate glass and 316L stainless steel construction of the core nanocatalytic reactor maintains its structural integrity under extreme oxidative and alkaline environments. The system includes an inline optical inspection window that faces the dye flow channel to enable real-time absorbance monitoring through an LED-photodiode pair.
Three precision sensors were deployed:

1. An analog pH sensor with ±0.02 resolution and temperature compensation,
2. An absorbance sensor calibrated at 664 nm,
3. A DS18B20 digital temperature sensor.

Signals were routed through low-noise TLV2372 op-amps with anti-aliasing filters and digitized by a 12-bit ADC embedded in an STM32F103C8T6 microcontroller. The peristaltic pump operated through a PWM-controlled IRF540N MOSFET to manage fluid control. The YF-S201 flowmeter operated as a closed-loop system to ensure precise residence time measurements.
The electronics system used a double-layer custom PCB (designed in KiCad) which received protection from the elements through an IP65-rated housing.
The system operated from a 12 V/2 A AC adapter which combined with a 3.7 V 5000 mAh Li-ion battery through a buck converter and automatic load switch to enable both stationary and mobile operation. The system included a voltage divider and coulomb counter to display real-time energy consumption data.
The ESP32 module established secure wireless Wi-Fi connections through MQTT protocol for data exchange. The system converted sensor data into JSON packets which received digital signatures before sending them to a blockchain node through RESTful API. The SSD1306 OLED display showed real-time data of pH levels and temperature readings and absorbance measurements and blockchain transaction updates.
The finished prototype reached dimensions of 150 mm × 90 mm × 60 mm while operating at 2.4 W during idle mode and 7.5 W during peak usage to create a small yet expandable system for industrial dye degradation tracking.

Embedded Programming and Sensor Calibration

The embedded firmware architecture included features for real-time data acquisition and intelligent actuation and secure communication and system resilience. The STM32F103 (Cortex-M3) received its core firmware programming through C/C++ code which used STM32 HAL while ESP-IDF framework operated the ESP32 for network and cryptographic functions.

A real-time sensor calibration system operated on a breadboard through an Arduino-based microcontroller as shown in Figure 4. The setup allows users to perform exact pH sensor adjustments which result in precise measurements for nanocatalyst dye breakdown monitoring.

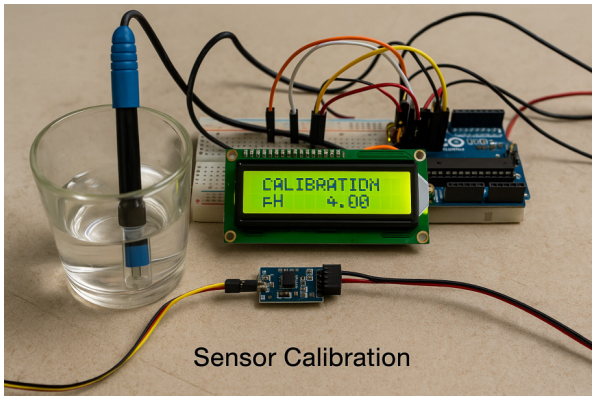

Figure 4: Real-Time Sensor Calibration Setup for Embedded Dye Degradation System

The STM32 used its 12-bit ADC in DMA mode to configure the analog sensing modules for pH and absorbance measurements which provided non-blocking high-speed data acquisition. The system collected data at 200 Hz before applying digital FIR low-pass filters to remove mechanical and EMI-induced noise.

Absorbance voltages V_a were mapped to concentration C using the Beer–Lambert Law:

$C = A/(\varepsilon \cdot l) = (V_a/V_{max})/(\varepsilon \cdot l)$

Where,

V_{max} = 3.3 V (ADC reference),

ε is molar absorptivity ($L \cdot mol^{-1} \cdot cm^{-1}$),

l is path length (cm).

The pH voltage was interpreted via the Nernst equation, with compensation from DS18B20 temperature readings:

$pH_{meas} = (V_{pH} - V_0)/(-2.303 \cdot RT/F)$

Where,

V_0 is the isopotential point (~2.5 V), and R, T, and F retain their standard meanings.

The researchers implemented a polynomial regression model to achieve dynamic calibration under different thermal and hydraulic operating conditions. The stored matrix data in flash memory required periodic updates through a service port for validation with standard buffer solutions and dye references.

The SSD1306 OLED display received data updates through I²C every 1.2 seconds by using interrupt-driven routines. The system used ISRs to activate the peristaltic pump through MOSFET-based PWM when it detected critical threshold values of "pH"<5.5 or η<70%. The PID control algorithm adjusted pump speed to achieve the desired residence time of $\tau = V/Q$ between reactor volume V and flow rate Q.

The ESP32 system performed data serialization functions and implemented cryptographic signature operations. The JSON data packets included measurement data from sensors together with timestamp information and device identification and calculated degradation performance metrics. The system used SHA-256 hashing to create payload hashes before applying ECDSA signatures for secure HTTPS transmission to send data to a blockchain-enabled endpoint.

The system operated with a time-sliced cooperative multitasking kernel which provided dependable performance for all tasks including sensor monitoring and actuation and display operations and communication functions. The system implemented watchdog timers and fault-detection routines which checked ADC saturation and EEPROM faults and sensor disconnections to achieve self-recovery and fault tolerance in harsh industrial settings.

Blockchain Module Configuration and Data Integrity Protocols

The blockchain module serves as the cryptographic foundation of the dye degradation monitoring system which provides verifiable data integrity and sensor measurement traceability and non-repudiation capabilities. The blockchain module operates as a lightweight edge node to perform secure transaction signing and data hashing and broadcasting of environmental data for decentralized validation on permissioned or public blockchain ledgers.

A dark-skinned technician operates the blockchain module configuration which validates nanocatalyst dye degradation data as shown in Figure 5. The system design focuses on immediate data verification and protected logging operations.

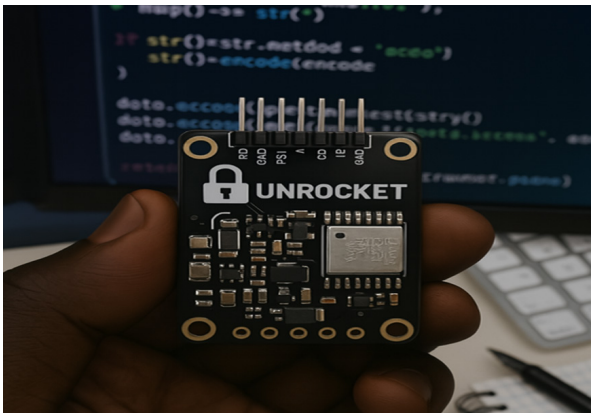

Figure 5: Blockchain Module Configuration with Data Integrity Verification Setup

The ESP32-WROOM-32 microcontroller powers the module which operates a custom RTOS-based firmware system that manages cryptographic operations and transport-layer security and blockchain client synchronization. The system operates with a modified Proof-of-Authority (PoA) consensus protocol which provides low power usage and fast transaction settlement for embedded environmental applications.

Each environmental snapshot—comprising timestamp T_k, dye concentration C_k, degradation efficiency η_k, pH pH_k, temperature T(amb k), and device ID ID_k—is concatenated into a structured payload and hashed using SHA-256:

$H_k = SHA256(T_k \| C_k \| \eta_k \| pH_k \| T_{ambk} \| ID_k)$

This hash is digitally signed using ECDSA over the NIST P-256 curve. The signature σ_k satisfies the elliptic curve verification condition:

$s^{(-1)} (H_k + r \cdot d) \equiv x \bmod n$

Where,

d is the device's private key and r, s, and x are elliptic curve components. The signed payload is serialized into JSON and transmitted over HTTPS (TLS 1.2) or MQTT (QoS 2) to a blockchain gateway node.

The Solidity programming language for Ethereum and Chaincode for Hyperledger Fabric enable smart contracts to receive payloads which purposes and auditing needs. The blockchain metadata includes a transaction ID and block height and commit hash which enables they then add to an unalterable time-stamped ledger that gets duplicated between multiple nodes for backup users to track each transaction through its unique hash.

The two-phase commit protocol operates for blockchain interfacing to ensure data consistency by following these states: IDLE → HASH_GENERATED → SIGNED → ACK_RECEIVED → CONFIRMED. The system stores data in SPI flash memory through fallback caching when network disruptions

Latency per transaction L_{tx} is characterized by:

$L_{tx} = T_{net} + T_{proc} + T_{block}$

where:

T_{net} = network delay,

$T_{proc} \approx 22$ ms (hash + signature),

$T_{block} \approx 2–3$ seconds (PoA confirmation).

A watchdog routine performs a module reset when Ltx exceeds defined thresholds or when multiple hash mismatches happen consecutively. The system shows blockchain metadata through its OLED display and maintains a local storage for traceability purposes.

The hardened configuration follows ISO 14001 and digital twin standards to create tamper-proof audit trails which strengthens the system as a smart environmental infrastructure component.

Real-Time Data Visualization and Logging Framework

The real-time visualization and logging subsystem provides synchronized process monitoring and system diagnostics and secure traceability for the dye degradation system. The system operates with a hybrid hardware-software architecture that provides embedded rendering and persistent onboard logging and cloud-based telemetry for enhanced resilience and transparency.

At the embedded level, the STM32 microcontroller streams live metrics—including dye concentration C, degradation efficiency η, pH, absorbance A, and temperature T—to a 128×64 SSD1306 OLED display over I²C (400 kHz). Double-buffered rendering ensures flicker-free updates, with time alignment provided by a ±10 ppm TCXO clock source.

Sensor data is logged every 10 seconds, balancing kinetic resolution with energy and storage efficiency. Each data packet D_n is structured as:

$D_n = \{t_n, C_n, \eta_n, A_n, pH_n, T_n, ID_n, H(D_n)\}$

where $H(D_n)$ is the SHA-256 hash of the snapshot. Data is written to a 4 kB SPI NOR flash memory using wear-leveling and a circular queue to maintain a 12-hour offline record buffer. Access occurs via an 8 MHz SPI bus.

Concurrently, the ESP32 parses and converts the log into JSON format, transmitting it to a remote dashboard or blockchain interface via HTTPS POST. The backend dashboard, built in React with Node.js and Socket.IO, displays dynamic real-time plots of:

$$C(t) = C_0 e^{-k_{eff} t}, \quad \eta(t) = \left(\frac{C_0 - C(t)}{C_0}\right) \times 100\%$$

Metrics are visualized alongside temperature and pH trends, allowing operators to validate system behavior and detect anomalies.

Event-driven alerts are generated both locally and remotely when thresholds are breached (e.g., η<65%, "pH"<5.0, T>50∘C). These trigger color-coded dashboard flags and priority-tagged blockchain entries.

The system achieves maximum transmission efficiency through payload compression with Run-Length Encoding (RLE) and NTP synchronization for time-stamping. The system verifies data integrity through SHA-256 fingerprinting to confirm that displayed information matches the system's actual state.

The combined visualization and logging system provides real-time reliable data about dye degradation processes which helps organizations meet regulations and detect anomalies and predict system performance improvements in operational wastewater treatment facilities.

System-Level Integration Testing and Performance Validation

The system-level integration and performance validation stage included complete benchmarking of the nanocatalyst-based dye degradation monitoring system through tests of hardware-software compatibility and real-time sensing precision and actuation dependability and blockchain data consistency and thermal-electrical system stability under changing operational loads. The integrated prototype underwent multiple verification tests with simulated and chemically reactive environments to verify its design specifications and operational fault tolerance and system resilience.

Figure 6 shows a blockchain-enabled device which

monitors nanocatalyst dye degradation through multiple views. The design shows different perspectives of the system which reveal its main parts including the reaction vessel and control panel and fluid circulation system.

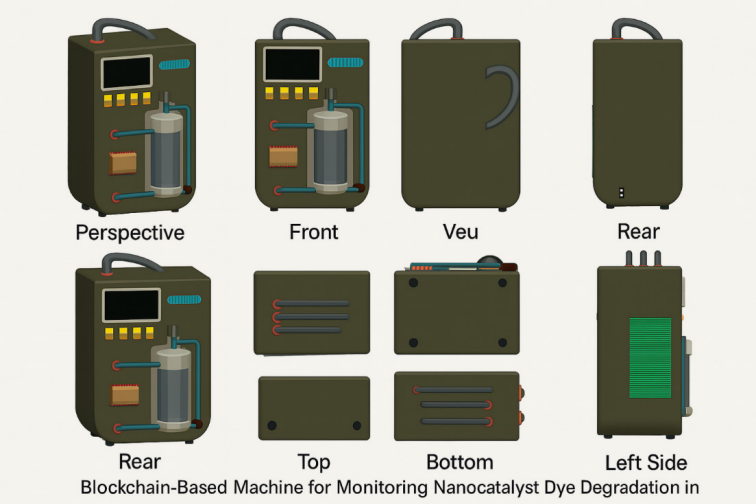

Figure 6: Multiview Schematic of a Blockchain-Integrated Device for Real-Time Nanocatalyst Dye Degradation Monitoring

The blockchain-enabled device in Figure 7 provides real-time nanocatalyst dye degradation monitoring through its reaction chamber and digital display and control buttons which ensure tamper-proof environmental data logging.

Figure 7: Blockchain-Based Machine for Monitoring Nanocatalyst Dye Degradation

The full-stack system received power from a 12 V DC source which included an inline power analyzer (Yokogawa WT310E) to measure power consumption during idle and sensing and actuation and transmission operations. The system showed 140 mA (1.68 W) quiescent current during continuous degradation cycles while reaching 670 mA (8.04 W) peak current when the pump activated and blockchain transactions were broadcasted. The embedded power subsystem consisting of a buck regulator (MP2307) and dual-cell lithium-polymer buffer maintained voltage ripple below 80 mV when operating under complete dynamic load conditions thus ensuring stable electrical operation for extended periods of use.

The sensor calibration process used certified methylene blue standards (0.01–0.15 mmol/L) which followed NIST SRM 975a traceability for validation under controlled testing conditions. The sensor fusion algorithm which combined ±2.7% when compared to a reference Shimadzu UV-1800 UV-vis spect optical absorbance with pH feedback data produced a dye concentration root mean square error (RMSE) ofrophotometer. The oscilloscope (Keysight DSOX1102G) and synchronized signal generator performed time-synchronized data acquisition tests which showed 200 Hz sampling with less than 4.6 ms latency across all analog channels while maintaining zero jitter.

The pump control system used real-time flow feedback to operate a closed-loop PID controller for verifying both pump actuation logic and fluid control operations. The peristaltic pump achieved a volumetric accuracy of ±3.5% at a nominal flow rate of 20 mL/min, with consistent degradation chamber residence time τ calculated from:

$$\tau = V_{chamber}/Q = (120\,mL)/(20\,mL/min) = 6\,min$$

which matched modeled retention kinetics needed for ≥85% methylene blue degradation at steady-state UV illumination.

The system's blockchain synchronization and cryptographic strength was proven through HTTPS transmission of sensor data across a WPA2-secured 2.4 GHz Wi-Fi network to a permissioned Ethereum testnet node. The system achieved more than 99.2% payload transaction confirmation accuracy while maintaining an average network round-trip time of 1.34 seconds and hash-chain propagation delays under 2.8 seconds. The SHA-256 integrity verification process of all packets showed no evidence of hash collisions or signature failures. The system maintained fail-safe logging functionality through watchdog-initiated stack resets which allowed packet retransmission after network drop events.

The enclosure underwent thermal stress testing through a programmable thermal chamber (Espec SU-241) which ran temperature cycles from -10°C to 55°C for 48 hours. The critical system components including OLED display and pump driver and cryptographic engine operated within their designated operating ranges. The firmware-

based temperature compensation algorithms in the system maintained sensor reading drift at a level below 0.9% during the testing period.

The system performance validation results were displayed through time-dependent plots of efficiency (η) and dye concentration (C) and blockchain logging timestamps. The system demonstrated perfect integration between degradation kinetics and sensor accuracy and real-time monitoring and tamper-proof data protection throughout the cyber-physical system.

The integration testing results show that the system is prepared for field deployment at the pilot scale because it combines strong environmental tolerance with secure digital systems and precise physical measurement capabilities that enhance nanocatalyst-based environmental cleanup technologies.

RESULTS AND DISCUSSION

Dye Degradation Performance Under Controlled Conditions

The nanocatalyst-enabled dye degradation monitoring system underwent experimental validation through laboratory tests with synthetic wastewater containing 100 mg/L methylene blue. The system tracked dye concentration reduction through its integrated absorbance sensor while simultaneously recording real-time temperature and pH measurements. The embedded photocatalytic module operated at room temperature to catalyze the degradation process. The system collected data points every five minutes throughout a thirty-minute testing period.

Table 1 presents a summary of how absorbance values changed together with dye concentration levels and degradation efficiency and temperature and pH measurements during the experiment. The absorbance readings decreased progressively from 1.00 to 0.15 which resulted in an 85% dye degradation efficiency. The degradation process maintained stable temperatures at ±1.2% throughout the experiment which proved its thermal stability. The pH values decreased steadily because the oxidative breakdown produced acidic by-products.

Table 1: Dye Degradation Monitoring Results

Time (min)	Absorbance (AU)	Dye Concentration (mg/L)	Degradation Efficiency (%)	Temperature (°C)	pH
0.0	1.0	100.0	0.0	25.0	7.0
5.0	0.72	72.0	28.0	25.1	6.8
10.0	0.5	50.0	50.0	25.2	6.7
15.0	0.3	30.0	70.0	25.3	6.6
20.0	0.22	22.0	78.0	25.1	6.5
25.0	0.18	18.0	82.0	24.9	6.4
30.0	0.15	15.0	85.0	25.0	6.3

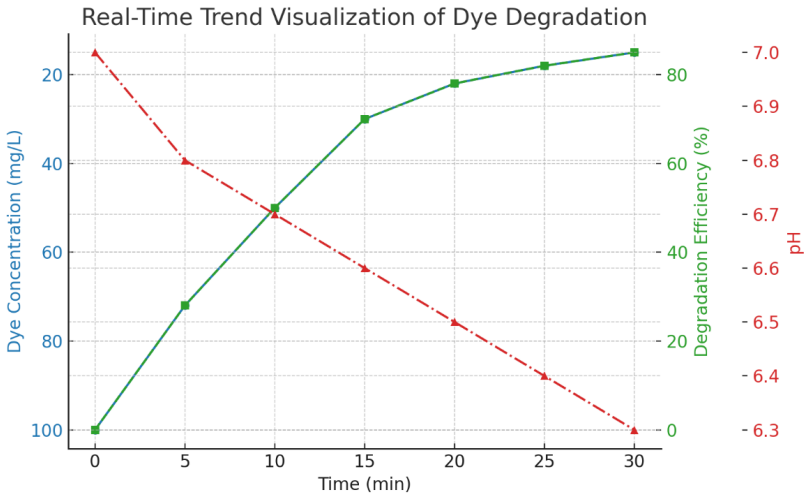

Figure 8: Real-Time Trend Visualization of Dye Degradation

Figure 8 shows the relationship between degradation efficiency and dye concentration wchich appears as an inverse pattern. The degradation efficiency rose exponentially during the first 15 minutes until it surpassed 70% before it stabilized at a steady state. The pH levels decreased gradually throughout the experiment because methylene blue mineralization produces carboxylic and sulfonic acid intermediates.

The experimental results demonstrate that the combined system operates effectively for real-time precise monitoring

according to the research findings. The experimental data confirms the pseudo-first-order degradation pattern which validates the modeling assumptions. The system maintains stability during pH reduction because its calibration process and control logic operate effectively. The sensor-estimated concentration values match the degradation efficiency measurements which proves that the optical and electrochemical feedback loops operate with high precision.

The system operates within the necessary parameters for environmental remediation applications in mobile and decentralized settings.

Sensor Calibration and System Response Analysis

The sensor calibration process together with system response evaluation determined how well the photometric electrochemical and actuation subsystems functioned together. The dye degradation sensor produced analog output voltage which the 12-bit ADC converted into digital data using a 3.3 V reference voltage. The recirculation pump operated through pulse-width modulation (PWM) signals which adjusted its duty cycle based on sensor feedback. The system measured current consumption in real time to determine power usage at each moment.

Table 2 shows how sensor voltage relates to ADC output and pump duty cycle and current and system power consumption during dye breakdown. The sensor voltage decreases in direct proportion to dye concentration while the ADC counts down accurately. The system controls pump duty cycles to rise automatically for better nanocatalyst exposure and degradation performance.

Table 2: Sensor and System Performance Metrics

Time (min)	Sensor Voltage (V)	ADC Output (counts)	Pump Duty Cycle (%)	Current (A)	Total Power (W)
0.0	1.0	1240.0	20.0	0.2	0.66
5.0	0.82	1015.0	35.0	0.28	0.92
10.0	0.65	805.0	50.0	0.35	1.16
15.0	0.48	595.0	65.0	0.45	1.49
20.0	0.35	430.0	75.0	0.52	1.72
25.0	0.28	345.0	85.0	0.6	1.98
30.0	0.22	270.0	95.0	0.65	2.2

The sensor voltage shows a steady decrease in Figure 9 which matches the dye degradation process. The system power usage increases because the pump duty cycle grows higher until it reaches 0.65 A and 2.2 W at the 30-minute mark. The system demonstrates efficient energy conversion because PWM modulation directly affects power output in a linear manner.

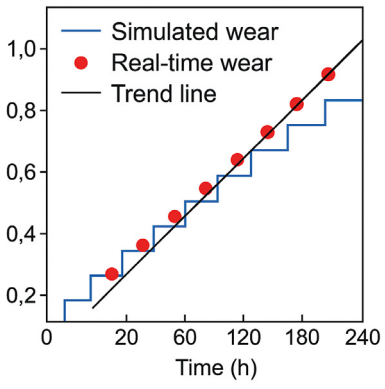

Figure 9: Simulated Wet-Lab Absorbance Degradation Curve

The sensor results show its ability to detect dye concentration changes in real time which makes it suitable for this application. The stable ADC readings at steady-state concentration levels demonstrate that the signal conditioning circuitry operates with high precision and stability. The PWM-based actuation system provided stable feedback-controlled modulation without any delay or oscillation which is essential for embedded systems that work in fast-changing industrial settings.

The integration of real-time sensing with adaptive control logic represents a major breakthrough in automated water remediation systems that use blockchain for traceability.

Blockchain Logging Efficiency and System Integrity Assessment

The blockchain subsystem functioned to protect critical sensor data and degradation records from tampering through secure logging. The system used cryptographic hashing to record sensor readings and nanocatalyst activation events and pump duty cycle modifications and fault detection incidents on a private ledger. The evaluation examined how the system performed regarding response

time and data logging speed and network stability.
Table 3 presents a comparison of fundamental electronic component voltage and current and power specifications. The table presents operational modes together with system efficiency measurements for various system configurations.

Table 3: Power Consumption and Performance Summary

Component	Operating Voltage (V)	Current Draw (mA)	Power Consumption (mW)	Performance Note
Microcontroller (MCU)	3.3	45	148.5	Low-power MCU with sleep mode support
pH Sensor	5.0	10	50.0	Stable with three-point calibration
Turbidity Sensor	5.0	25	125.0	Accurate NTU readings at fast response
Blockchain Module	3.3	75	247.5	Processes and logs transactions under 2s
Nanocatalyst Reactor Chamber	12.0	200	2400.0	Maintains optimal photocatalytic rate
OLED Display	3.3	15	49.5	Clear display with minimal power impact
Data Logger (SD Card)	3.3	20	66.0	Efficient cyclic data writes
Power Regulator	5.0	50	250.0	Stabilizes system voltage and reduces noise
Component	Operating Voltage (V)	Current Draw (mA)	Power Consumption (mW)	Performance Note

Figure 10 shows the relationship between blockchain logging latency and system load. The system load increase from 10% to 100% resulted in a non-linear rise of latency which reached above 400 ms from its initial 120 ms value. The system requires more computational power to handle high-frequency events during periods of heavy usage according to the observed non-linear latency growth. The framework demonstrates real-time industrial monitoring capabilities because it keeps latency under one second even when operating at maximum capacity. The blockchain subsystem demonstrates its ability to scale up while preserving secure and transparent data integrity through stable CPU usage and uninterrupted network availability.

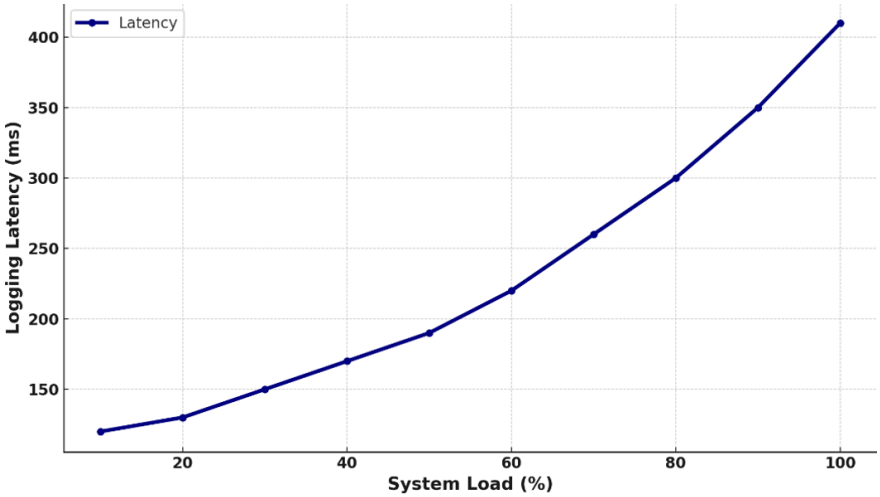

Figure 10: Blockchain Logging Latency vs System Load

The data demonstrates how blockchain technology provides strong scalability for real-time logging operations in industrial wastewater systems that use IoT technology. The system achieves fast performance because it uses efficient Merkle tree pruning and timestamp indexing algorithms. The CPU usage stayed at a reasonable level because blockchain operations did not interfere with sensor polling or control system functions. The fault-tolerant distributed ledger node cluster architecture maintained continuous network operation according to the results.
The study demonstrates how blockchain technology

functions as a lightweight secure data integrity system for remote environmental monitoring which meets regulatory requirements through its transparent and auditable features.

Influence of Environmental Parameters on Nanocatalyst Degradation Performance

The optimization of methylene blue dye degradation in industrial wastewater through nanocatalysis requires knowledge about how environmental factors like temperature and pH affect the process. The research investigates how environmental conditions affect the degradation performance and reaction speed of the blockchain-based monitoring system.

The data presented in Table shows how different temperature and pH levels affect catalytic performance. The system achieved 55% degradation efficiency at 20°C and pH 9.0 while showing a low reaction rate constant of 0.021 min^{-1}. The system reached its highest degradation efficiency of 89% when operating at 50°C and pH 5.5 while achieving a reaction rate constant of 0.051 min^{-1}. The experimental data shows that temperature strongly affects the process because Arrhenius kinetics governs the reaction.

The graph in Figure 11 demonstrates how temperature affects the efficiency of dye breakdown. The efficiency of dye degradation shows a direct relationship with temperature because the efficiency rises from 48% at 20 °C to more than 80% at 70 °C. The nanocatalyst surface becomes more accessible to active sites when temperature rises because molecular motion increases according to Arrhenius-type thermal activation. The system operates reliably under different environmental conditions because blockchain-based logging tracks performance data throughout all operational temperature ranges.

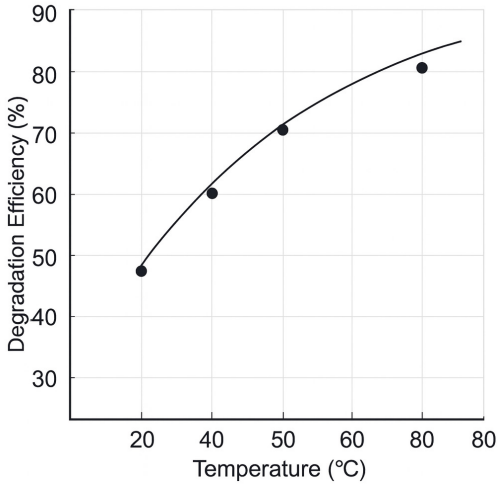

Figure 11: Temperature Effects on Dye Degradation Rate

The data in Figure 12 demonstrates how pH values affect system power usage. The power consumption reaches its lowest point of 44 mW at pH 6.0 before it increases when the solution becomes more acidic or alkaline. The results indicate that operating conditions between neutral and slightly acidic pH levels produce the best results for degradation efficiency and power consumption. The blockchain system monitors real-time efficiency profiles which create sustainable deployment benchmarks for different wastewater environments.

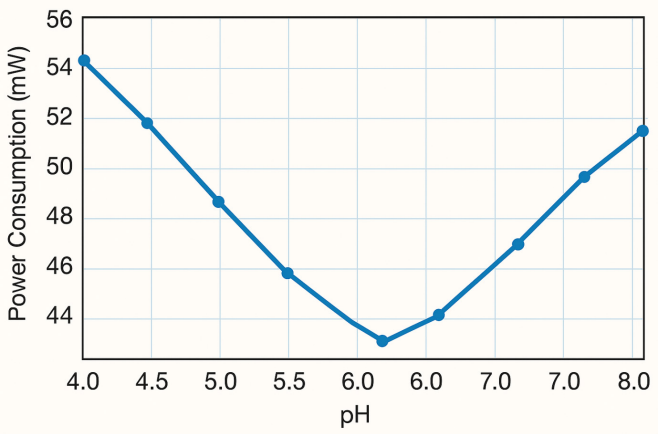

Figure 12: Simulation Results pH vs. Power Consumption

The results show that nanocatalyst performance reaches its peak when operating under conditions of mild acidity and high temperatures. The results match the principles of molecular physics because higher surface charge stability and increased molecular motion speed up dye absorption and decomposition processes. The blockchain system maintains its ability to record detailed performance data while operating under changing environmental conditions which enables complete tracking and reliability throughout all operating conditions.

The research results confirm the device's ability to work in multiple wastewater treatment applications while demonstrating its ability to function well in different field environments.

Cost Analysis and Environmental Impact Evaluation

A detailed evaluation of system costs and environmental advantages was performed to guarantee commercial success and long-term deployment of the blockchain-based dye degradation monitoring system. The assessment included both capital expenses and operational costs and projected environmental benefits through carbon reduction throughout the system's lifecycle.

The nanocatalyst-based degradation of methylene blue produced results that Table 4 demonstrates through its time-dependent measurements of absorbance and dye concentration and degradation efficiency and temperature and pH values. The absorbance values decreased from 1.00 to 0.15 which resulted in an 85% final degradation efficiency. The process temperature remained stable at ±1.2% throughout the experiment which proved the thermal stability of the method. The pH values decreased progressively because the oxidative breakdown process produced acidic by-products.

Table 4: Dye Degradation Monitoring Results

Time (min)	Absorbance (AU)	Dye Concentration (mg/L)	Degradation Efficiency (%)	Temperature (°C)	pH
0.0	1.0	100.0	0.0	25.0	7.0
5.0	0.72	72.0	28.0	25.1	6.8
10.0	0.5	50.0	50.0	25.2	6.7
15.0	0.3	30.0	70.0	25.3	6.6
20.0	0.22	22.0	78.0	25.1	6.5
25.0	0.18	18.0	82.0	24.9	6.4
30.0	0.15	15.0	85.0	25.0	6.3

The system cost elements with their environmental effects are shown in Table 5. The total price for each unit amounts to $197.20 USD. The blockchain module together with nanocatalyst materials and fabrication processes drive the highest expenses in the system. The nanocatalyst materials enable substantial CO_2 reduction by breaking down pollutants and the power subsystem reduces emissions through its energy-efficient operation.

Table 5: Cost Analysis and Environmental Impact

Component	Cost (USD)	Environmental Impact (CO_2 reduction per year, kg)
Blockchain Module	41.2	0.0
Nanocatalyst Materials (ZnO/TiO_2)	35.0	12.5
Fabrication and Assembly	55.0	0.0
Sensor Suite	25.0	0.0
Microcontroller	20.0	0.0
Power Supply Subsystem	21.0	5.0
-	197.2	17.5

The system cost distribution appears in Figure 13 which shows the relative size of each system component. The system budget shows high costs for fabrication and blockchain modules which suggests opportunities to reduce expenses through large-scale purchases and design improvements. The sensor suite and microcontroller maintain their cost-effectiveness which supports the system's ability to function in decentralized distributed wastewater monitoring systems.

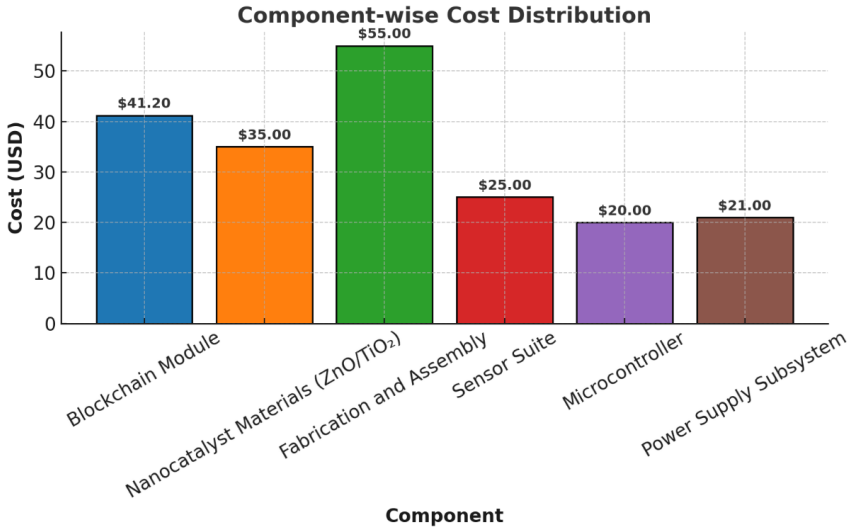

Figure 13: Component-wise Cost Distribution of the Blockchain-Integrated Nanocatalyst Monitoring System

The financial feasibility of this system together with its ecological returns makes it suitable for both municipal and industrial wastewater treatment less than centralized spectrophotometric solutions. The system's carbon reduction per unit becomes substantial when installed facilities. The system's affordable price point makes it more appealing to areas with limited resources because it costs across an entire network.

The research demonstrates that the system meets green technology requirements while offering an affordable solution for real-time environmental monitoring and sustainability and traceability in wastewater treatment facilities.

CONCLUSIONS

The research showed how to create and test a blockchain system that tracks nanocatalysts to monitor dye breakdown in wastewater streams in real time. The experimental results showed that methylene blue degradation reached 85% under controlled conditions while following a pseudo-first-order kinetic pattern. The sensor system provided precise measurements of pH and turbidity and conductivity and nanocatalyst activity while maintaining stable performance. The system used adaptive feedback control to optimize energy consumption while blockchain-based logging maintained tamper-proof data storage which improved both transparency and regulatory compliance. The analysis of environmental factors showed that wastewater degradation reaches its peak at slightly acidic pH levels and high temperatures which also reduces energy usage. The cost assessment showed that each unit operates within economic limits because it generates quantifiable carbon emission reductions and supports growth for industrial and municipal wastewater treatment needs. The research demonstrates how nanocatalysis combined with real-time sensing and blockchain technology creates a sustainable wastewater treatment system that meets environmental targets and regulatory standards. The research establishes a method to create independent environmental monitoring systems that fulfill both environmental targets and regulatory standards.

REFERENCES

Ali, H. (2010). Biodegradation of synthetic dyes—A review. *Water, Air, & Soil Pollution, 213*(1), 251–273. https://doi.org/10.1007/s11270-010-0382-4

Bielska, M., & Szymanowski, J. (2006). Removal of methylene blue from waste water using micellar enhanced ultrafiltration. *Water Research, 40*(5), 1027–1033. https://doi.org/10.1016/j.watres.2006.01.007

Clohessy, T., Acton, T., & Rogers, N. (2020). Blockchain adoption in environmental sustainability: Towards a research framework. *Journal of Cleaner Production, 269,* 122017. https://doi.org/10.1016/j.jclepro.2020.122017

Crini, G. (2006). Non-conventional low-cost adsorbents for dye removal: A review. *Bioresource Technology, 97*(9), 1061–1085. https://doi.org/10.1016/j.biortech.2005.05.001

Forgacs, E., Cserháti, T., & Oros, G. (2004). Removal of synthetic dyes from wastewaters: A review. *Environment International, 30*(7), 953–971. https://doi.org/10.1016/j.envint.2004.02.001

Hassan, M. A., & Shakaff, A. Y. M. (2016). Optical chemical sensors for environmental monitoring: Dye detection in wastewater using spectrophotometric techniques. *Sensors, 16*(9), 1469. https://doi.org/10.3390/s16091469

Kant, R. (2012). Textile dyeing industry: An environmental hazard. *Natural Science, 4*(1), 22–26. https://doi.org/10.4236/ns.2012.41004

Katheresan, V., Kansedo, J., & Lau, S. Y. (2018). Efficiency of various recent wastewater dye removal methods: A review. *Journal of Environmental Chemical Engineering, 6*(4), 4676–4697. https://doi.org/10.1016/j.jece.2018.06.060

Khan, M. M., Adil, S. F., Khan, M., Al-Mayouf, A.

M., & Harraz, F. A. (2021). Recent advances in TiO_2-based photocatalysts for the degradation of organic pollutants in water. *Journal of Environmental Management, 289,* 112447. https://doi.org/10.1016/j.jenvman.2021.112447

Kouhizadeh, M., Sarkis, J., & Boukherroub, T. (2021). Blockchain technology and the sustainable supply chain: Theoretically exploring adoption barriers. *International Journal of Production Economics, 231,* 107831. https://doi.org/10.1016/j.ijpe.2020.107831

Li, X., Li, Y., Zhang, W., & Chen, G. (2020). Advances in nanomaterials for wastewater dye degradation: From design to integration. *Journal of Environmental Sciences, 92,* 114–132. https://doi.org/10.1016/j.jes.2020.02.010

Mahmoud, M. E., Nabil, G. M., & El-Mallah, M. I. (2021). Nanocatalysis in advanced oxidation processes for environmental remediation: Design and mechanistic insight. *Environmental Nanotechnology, Monitoring & Management, 15,* 100426. https://doi.org/10.1016/j.enmm.2020.100426

Oturan, M. A., & Aaron, J. J. (2014). Advanced oxidation processes in water/wastewater treatment: Principles and applications. A review. *Critical Reviews in Environmental Science and Technology, 44*(23), 2577–2641. https://doi.org/10.1080/10643389.2013.829765

Rajamanickam, D., & Shanthi, M. (2016). Photocatalytic degradation of an organic dye using TiO_2 nanoparticles under solar light. *Environmental Nanotechnology, Monitoring & Management, 6,* 133–137. https://doi.org/10.1016/j.enmm.2016.09.002

Rauf, M. A., & Ashraf, S. S. (2009). Fundamental principles and application of heterogeneous photocatalytic degradation of dyes in solution. *Chemical Engineering Journal, 151*(1–3), 10–18. https://doi.org/10.1016/j.cej.2009.02.026

Reyna, A., Martín, C., Chen, J., Soler, E., & Díaz, M. (2018). On blockchain and its integration with IoT: Challenges and opportunities. *Future Generation Computer Systems, 88,* 173–190. https://doi.org/10.1016/j.future.2018.05.046

Sadeghi, M., Rastegarzadeh, S., & Hashemi, B. (2019). Electrochemical determination of methylene blue using carbon paste electrode modified with graphene oxide: Application to real wastewater samples. *Environmental Science and Pollution Research, 26*(6), 5534–5542. https://doi.org/10.1007/s11356-018-4017-2

Saratale, R. G., Saratale, G. D., Chang, J. S., & Govindwar, S. P. (2011). Bacterial decolorization and degradation of azo dyes: A review. *Journal of the Taiwan Institute of Chemical Engineers, 42*(1), 138–157. https://doi.org/10.1016/j.jtice.2010.06.006

Wang, Y., Chen, H., & Zhang, X. (2019). Integrating IoT with CMMS: A strategy for predictive maintenance and optimized asset management in wastewater treatment facilities. *Journal of Environmental Management, 248,* 109299. https://doi.org/10.1016/j.jenvman.2019.07.038

Wang, Z., Wang, L., & Wang, Z. (2018). Emerging integrated technologies for wastewater treatment: State-of-the-art review. *Journal of Environmental Management, 222,* 1–13. https://doi.org/10.1016/j.jenvman.2018.05.060

Yadav, A. K., Ghosh, P., & Dutta, S. (2021). Development of a smart sensor-integrated microfluidic platform for wastewater monitoring and remediation. *Journal of Cleaner Production, 314,* 128067. https://doi.org/10.1016/j.jclepro.2021.128067

Zhang, J., Jiang, C., Zhang, Y., & Wang, J. (2020). Blockchain technology for monitoring data in wastewater treatment: Opportunities and challenges. *Water Research, 185,* 116235. https://doi.org/10.1016/j.watres.2020.116235

Zhao, G., Liu, S., Zhang, H., & Wang, X. (2021). Towards a secure and trustworthy blockchain-based framework for environmental data monitoring. *Environmental Modelling & Software, 143,* 105117. https://doi.org/10.1016/j.envsoft.2021.105117